NASA TECHNICAL NOTE

NASA TN D-5495

$\mathcal{C}. \, 1$

A LIMB RADIANCE CALCULATION APPROACH FOR MODEL ATMOSPHERES CONTAINING HORIZONTAL GRADIENTS OF TEMPERATURE AND PRESSURE

by Richard E. Davis

Langley Research Center
Langley Station, Hampton, Va.

| 1. Report No. | 2. Government Accession No. | 3. Recipient's Catalog No. |
| NASA TN D-5495 | | |

4. Title and Subtitle	5. Report Date
A LIMB RADIANCE CALCULATION APPROACH FOR MODEL ATMOSPHERES	October 1969
CONTAINING HORIZONTAL GRADIENTS OF TEMPERATURE AND PRESSURE	6. Performing Organization Code

| 7. Author(s) | 8. Performing Organization Report No. |
| Richard E. Davis | L-6775 |

| | 10. Work Unit No. |
| | 125-17-07-08-23 |

9. Performing Organization Name and Address	11. Contract or Grant No.
NASA Langley Research Center	
Hampton, Va. 23365	
	13. Type of Report and Period Covered

12. Sponsoring Agency Name and Address	Technical Note
National Aeronautics and Space Administration	
Washington, D.C. 20546	
	14. Sponsoring Agency Code

15. Supplementary Notes

16. Abstract

A method is developed, using a numerical limb radiance computational model for the 14- to 16-micron CO_2 band, that accounts for the fact that real atmospheres strictly never show the spherically symmetric temperature and pressure stratification that is normally assumed in the calculations of limb radiance. Equations incorporating the effects of horizontal gradients are given, and tests performed with a modified numerical radiance computational program are described. Some examples of the application of the method are given. An improvement in the computational accuracy is achieved by the new method. This result is significant under winter conditions when strong latitudinal temperature gradients exist in the middle and polar latitudes.

17. Key Words Suggested by Author(s)	18. Distribution Statement
Limb radiance	Unclassified – Unlimited
CO_2 limb	
Radiance profile	
Tangent height	

| 19. Security Classif. (of this report) | 20. Security Classif. (of this page) | 21. No. of Pages | 22. Price* |
| Unclassified | Unclassified | 36 | $3.00 |

A LIMB RADIANCE CALCULATION APPROACH
FOR MODEL ATMOSPHERES CONTAINING HORIZONTAL GRADIENTS
OF TEMPERATURE AND PRESSURE

By Richard E. Davis
Langley Research Center

SUMMARY

A method is developed, using a numerical limb radiance computational model for the 14- to 16-micron CO_2 band, that accounts for the fact that real atmospheres strictly never show the spherically symmetric temperature and pressure stratification that is normally assumed in the calculations of limb radiance. Equations incorporating the effects of horizontal gradients are given, and tests performed with a modified numerical radiance computational program are described. Some examples of the application of the method are given. An improvement in the computational accuracy is achieved by the new method. This result is significant under winter conditions when strong latitudinal temperature gradients exist in the middle and polar latitudes.

INTRODUCTION

The use of horizon-sensing systems for attitude determination and control has been a feature of spacecraft almost since the beginning of space flight. The infrared region of the spectrum has received the most attention in horizon-sensor design, primarily because sensors operating in that region are useful in both the day and night parts of an orbit. In the infrared region, the absorption bands of carbon dioxide, water vapor, and ozone have been considered in sensor design. Of these gases, carbon dioxide seems to be favored at this time, because it is assumed to have uniform worldwide concentration up to very high altitudes; this condition is definitely not true for water vapor and ozone. Because this uniform absorber concentration of carbon dioxide should result in less variability in the limb (defined as the region of contrast between the cold of space and the thermal emissions of a planet and its atmosphere), theoretical calculations of the radiance of the limb in the 14- to 16-micron band have been performed or reported by several investigators. (See refs. 1 to 12.) High-quality experimental measurements of 14- to 16-micron limb radiances have been made, and these results have been compared with theoretical predictions for the atmospheric conditions existing at the times of the experiments. (See refs. 13 and 14.) The predictions have for a summer flight

(ref. 13) agreed well enough with observation to establish the basic soundness of limb radiance theory. In reference 14, however, the presence of strong horizontal gradients of temperature, as typically occur in the middle or subpolar latitudes in winter, violated a fundamental assumption upon which the radiance modeling was based; therefore, a meaningful comparison of the theory with results was not possible. The fundamental assumption referred to here and employed in all investigations before this one is that the model atmospheres employed have spherical symmetry. This assumption means that temperature and pressure in the model atmosphere vary only in the vertical and are changing negligibly over their region of application with latitude and longitude. This assumption is not too far in error for certain situations. In reference 13, for example, horizontal gradients were very small; theory agreed well with experiment. In the winter case reported as reference 14, the assumption of spherical symmetry was badly in error, and as the gradients existing in that instance were by no means unusual, it was obvious that the radiance modeling approach should be modified to remove the restrictive assumption of spherical symmetry. Therefore, in the present investigation, the conditions existing in an atmosphere containing horizontal temperature and pressure gradients were defined, in conformity with the assumption of hydrostatic equilibrium, by linear equations. The equations are presented in such a form that they may readily be applied by any investigator to the modification of his own limb radiance calculation program. The radiance calculation program in use at Langley Research Center (ref. 11) was modified by the inclusion of these equations to simulate the presence of horizontal temperature and pressure gradients. The mathematical description of including the horizontal gradients of temperature and pressure, the testing of the new model and its application to various sample cases are included in this paper.

SYMBOLS

C_1 constant, 1.1909×10^{-5} erg-centimeter^2/second-steradian

C_2 constant, 1.4389 centimeters-degrees

g magnitude of acceleration due to gravity, m-sec^{-2}

H tangent height, kilometers

J_ν source function, watts/meter^2-steradian-centimeter^{-1}

k Boltzmann constant, 1.3803×10^{-23} joule-deg^{-1}

m	molar weight of air, kg
N	radiance, watts/meter^2-steradian
N_ν	spectral radiance, watts/meter^2-steradian-centimeter^{-1}
p	pressure, millibars
p_r	reference pressure, millibars
S_p	constant
S_t	constant
s	distance along line of sight, kilometers
s_o	distance to opacity along line of sight, kilometers
T	temperature, kelvins
$\overline{T}$	average temperature, kelvins
W_ν	spectral radiant emittance, watts/meter^2-centimeter^{-1}
Z	altitude, kilometers
α_c	angular subtense of tangent point with respect to line CC' (see fig. 1(b)), degrees
α_r	angular subtense of arbitrary atmosphere used to compute the γ_p value (see fig. 1(b)), degrees
α_s	angle subtended by middle of shell s, on part of line of sight near the observer, with respect to reference line CC' (see fig. 1), degrees
β_s	counterpart of α_s, on part of line of sight more distant than tangent point from observer (see fig. 1), degrees
γ_H	horizontal gradient of temperature, kelvins/degree great circle

γ_p horizontal gradient of pressure, millibars/degree great circle

τ transmittance, dimensionless

ν wave number, centimeter^{-1}

Subscripts:

1   denotes shell 1

s   denotes any shell

BACKGROUND

Since early in the 1960 decade, both theoretical and experimental earth-limb radiance profiles have been obtained. Reference 1 is a recent summary of both theoretical and experimental results concerning infrared horizon definition. The theoretical work appears in references 2 to 12. References 13 to 22 are sources of experimental horizon radiance data. Of these, references 13, 14, 19, and 20 describe experiments having angular resolution and accuracy sufficient to show the effects of errors or approximations in the computational models employed. References 13, 14, and 19 represent the most thorough attempts to date to compare observed horizon radiance profiles with analytical profiles, and furthermore, are the only experiments to employ simultaneous meteorological balloon and rocket measurements in an effort to define as accurately as possible the input conditions for the analytical radiance model, that is, the actual atmospheric conditions at the time of the experiment. The radiative transfer theory background essential to understanding of the present work is summarized briefly in appendix A.

There are two main reasons that it is necessary to include the effect of horizontal temperature and pressure gradients in the transfer equation.

(1) As discussed in reference 14, the computational approach based on spherical symmetry has proven to be inadequate under some winter conditions. It is extremely important to remove the restriction of spherical symmetry so that scientifically profitable investigations may proceed, for example, toward the evaluation of various absorption models which may be used in numerical limb radiance models on a worldwide basis.

(2) There is considerable engineering interest in using the infrared radiance signature of the earth as a navigational reference for spacecraft in near-earth space. All analytical investigations of the stability of the infrared horizon, as located with the use

4

of various horizon detection logic techniques, have been accomplished with the use of radiance models which assume the absence of horizontal gradients in their input atmospheres. The results of these investigations may be somewhat misleading, because real atmospheres will include gradients. It is important for horizon-sensor designers to know the logic techniques that are most insensitive to the presence of strong gradients.

BASIC GEOMETRY OF PROBLEM

In previous approaches (for example, refs. 11, 13, and 14), the altitude of a spherical shell uniquely specified its temperature and pressure. In this problem these variables depend upon the location of the point of interest on the earth. The geometry is shown in figure 1. For simplicity, discussion is confined to the case in figure 1(a) in which the tangent height H is equal to zero. Figure 1(b) is included to describe the slightly more complicated situation which occurs when H is larger than zero. The line CC' defines a radius vector along which the model atmosphere is defined; that is, with each altitude along the radius vector CC' is associated a pressure $p(Z)$ and a temperature $T(Z)$. Consider a line of sight extending from the satellite and tangent to the earth at point O on the line CC'. In shell 1, the line of sight (LOS) intercepts the geometric center of the shell at altitude Z_1, lying α_1 great circle degrees from CC'. When no horizontal gradients exist within the shell of altitude Z_1, the temperature and pressure at that altitude are independent of position over the earth. This approximation is the spherical approximation that has been used in previous models.

Effects of Absence of Symmetry

The consequences of assuming that the body of atmosphere traversed by the line of sight has spherical symmetry may be understood from an example. To appreciate the reason for the importance of geographic separation, the temperature of a shell at 80 km is considered. It can be shown, where $H = 0$, that the point where the line of sight intersects this shell is removed geographically 9° from the line of reference CC'. If no temperature gradient exists, this separation causes no problems. But if one were to exist of magnitude 0.3 kelvin per degree of great circle (a physically realistic estimate), the temperature at the point where the line of sight crosses 80 km would differ 2.7 kelvins from the temperature at 80 km along the reference atmosphere line CC'. Consideration of well-known model atmospheres, given in reference 23 for sample summer and winter conditions, leads to an appreciation of the size of the temperature differences to be expected at the 80-km level. For a sample summer condition, with the line of sight pointing northward, and using the 15° N and the 30° N model atmospheres for July (ref. 23), the temperature change would be only 2.6 K. On the other hand, to approximate a typical severe gradient situation for winter, the 45° N and 60° N model atmospheres for January, from the same reference, may be used to yield a temperature change of 8.3 K at 80 km. Thus it is emphasized that the existence of gradients causes the

atmospheric conditions encountered for each shell along the line of sight to be significantly different from those defined vertically along the line CC'. For the shells lower than 80 km, the angles will obviously be smaller than 9°. However, the energy contribution from the lower altitude shells, where the atmosphere is denser, is much greater and a difference in temperature caused by such gradients will therefore have a larger effect on the radiance observed, although the angular separations of these shells from the line CC' are smaller than that of the shell at 80 km.

<center>Effect of Satellite Altitude</center>

In previous investigations, the assumption of spherical symmetry made it unnecessary to consider effects of satellite altitude. Since for this investigation the assumption has been removed, a small additional effect due to satellite altitude needs consideration. The geometry changes with the choice of tangent height and satellite altitude so that the tangent height occurs at a geographic location α_c great circle degrees separated from CC'. (See fig. 1(b).) For instance, for a satellite altitude of 500 km and a tangent height of 80 km, α_c is 1.87^O. For a tangent height of zero, α_c is, of course, 0°. If the satellite altitude is 1000 km, α_c becomes 1.32^O for a tangent height of 80 km. One should note that CC' is always defined by the vertical through the tangent point for H = 0, but the orientation of the line CT is dependent upon both satellite altitude and tangent height. If the satellite altitude increases to infinity, α_c for all tangent heights decreases to zero or all tangent heights lie along the line CC'. The importance of the geographic location of that shell corresponding to the tangent height lies in the large contribution of the gas in this shell to the magnitude of overall radiance for this tangent height for tangent height altitudes in excess of 20 km. Where large horizontal temperature gradients exist within this shell, the exact location of the tangent height point is very important in determining the effective temperature of the shell. Since previous analysts could ignore the effects of satellite altitude because no gradients existed, it was felt necessary to include an option for incorporating actual satellite altitudes into the revised radiance computation program to compensate for the small angular differences in location of the tangent-height points.

To determine the horizontal gradients of temperature and pressure in the atmosphere up to 80 km, some familiarity with the meteorological analyses and data available is necessary. These products and their use are described briefly in appendix B.

<center>MATHEMATICAL REPRESENTATION OF THE HORIZONTAL PRESSURE

AND TEMPERATURE GRADIENTS</center>

By using the meteorological analysis techniques described in appendix B, a cross-sectional analysis for the time and geographic area of interest is prepared. From the

cross section, one determines the temperature gradients by inspection. The gradient is defined as γ_H degrees per unit great circle angle in the direction of the observer, and in the work done for this paper has been represented as a linear function of angular distance in the shell from line CC'. In the general case, the line of sight passes through the atmosphere both on the near and far sides of the tangent height point, and corresponding to each shell altitude, there are two values of temperature — one on the near side, and one on the far side. The temperatures on the near and far sides are calculated from

$$T(Z_s)_{near} = T_0(Z_s) + \gamma_H(Z_s) \, \alpha_s(Z_s) \, S_t \tag{1}$$

$$T(Z_s)_{far} = T_0(Z_s) + \gamma_H(Z_s) \, \beta_s(Z_s) \, S_t \tag{2}$$

where $T_0(Z_s)$ is the temperature at altitude Z_s of the reference atmosphere, the vertical profile of which is defined along the line CC', γ_H is the previously mentioned horizontal-temperature gradient, α_s is the angular distance the shell at Z_s on the near side is distant from the reference line, β_s is the corresponding angle on the far side for the particular shell, and S_t is +1 if the temperature is generally increasing toward the observer or -1 if the temperature is generally decreasing.

Pressure is calculated by the following stepwise procedure:

(1) The vertical profile of pressure along the line CC' is constructed in accordance with hydrostatic equilibrium; that is, $p(Z_1)$ the pressure at altitude Z_1 is related to $p(Z_0)$ the pressure at altitude Z_0 by

$$p(Z_1) = p(Z_0) \, \exp - \frac{m}{k} \int_{Z_0}^{Z_1} \frac{g(Z) \, dZ}{\overline{T}(Z)} \tag{3}$$

where $\overline{T}(Z)$ is the mean temperature between altitudes Z_0 and Z_1 which is obtained by

$$\overline{T}(Z) = \frac{T(Z_0) + T(Z_1)}{2} \tag{4}$$

(2) The temperature profile at an arbitrary angle α_r away from CC' is derived from the cross-sectional analysis. This derivation is made to establish a base line over which a gradient of temperature can be calculated for each altitude.

(3) The base pressure existing at this new location is used as a starting point for the hydrostatic buildup of pressure by employing the temperatures found in step (2). In this way, a reference pressure $p_r(Z_s)$ is defined for each shell altitude Z_s at the reference location.

7

(4) From step (3), one now has two vertical profiles of pressure between which the pressure at any arbitrary point along the line of sight can be determined for the shell altitude Z_S by the following equations:

$$\gamma_p(Z_S) = \frac{p_r(Z_S) - p_o(Z_S)}{\alpha_r} \tag{5}$$

$$p(Z_S)_{near} = p_o(Z_S) + S_p \gamma_p(Z_S)\, \alpha_s(Z_S) \tag{6}$$

$$p(Z_S)_{far} = p_o(Z_S) + S_p \gamma_p(Z_S)\, \beta_s(Z_S) \tag{7}$$

where $\gamma_p(Z_S)$ is the horizontal gradient of pressure in millibars per degree of great circle at altitude Z_S, $p_r(Z_S)$ is the "reference pressure" at altitude Z_S which was calculated in step (3), $p_o(Z_S)$ is the pressure along CC' at latitude Z_S, and S_p is +1 if the sea-level pressure is increasing toward the observer or -1 if the pressure is decreasing. Only model and reference-location atmospheres are in strict hydrostatic equilibrium; the interpolated points have only approximate equilibrium.

DESCRIPTION OF ORIGINAL AND REVISED MODELS

The numerical radiance computation model used as the starting point for the implementation of the modifications which are the subject of this paper is that which is in general use at Langley Research Center, and which is described comprehensively in reference 11. The salient features of this model are:

Spectral region of interest, 600 to 725 cm^{-1}

Absorption data, Plass or Elsasser absorption model (ref. 11)

Input altitude range, arbitrary

Number of shells, arbitrary

Option to include H_2O and/or O_3 absorption (Elsasser data)

Refraction option

Option to account for lack of thermal equilibrium

Doppler broadening option

Ability to simulate effects of various filters

As a result of the work which has been performed under the present study, and which has been described in previous sections of this report, the following additional options are now available:

8

(1) The observer can be placed at an infinite or any arbitrary finite altitude

(2) Horizontal temperature gradients can be specified as:

    (a) Zero at all altitudes

    (b) Either positive or negative in the direction of the observer, and variable as a function of tangent height

(3) The surface pressure gradient can be specified as:

    (a) Zero

    (b) Either positive or negative in the direction of the observer

(4) The temperature and pressure for each shell along the line of sight may be printed out if desired. In cases where the line of sight includes shells from both in front of and beyond the tangent altitude, there are two pressures and temperatures corresponding to each shell altitude, but the corresponding correct values are printed out in the order of increasing distance from the observer.

Option (2(b)) is used to simulate the effects, for example, of looking northward in winter toward colder temperatures. This option could also be used to simulate the effects when the instrument looks southward. The results obtained from looking northward and looking southward could be used in horizon-sensor simulation programs to predict the magnitude of error in location of the local vertical. Option (3(b)) enables the presence of high- or low-pressure weather systems to be simulated. Thus by appropriate selections of the magnitudes and signs of the gradients, many realistic temperature and pressure fields may be simulated for radiance computation purposes.

It was desirable to check out the new computational model to determine whether it gave reasonable answers under various test conditions. Two tests were performed and these tests are described in detail in appendix C. The computation time typically required is also described there.

EXAMPLES OF THE UTILIZATION OF THE TECHNIQUE ON VARIOUS METEOROLOGICAL SITUATIONS

To demonstrate the utility of the technique, three examples are given. The first of these deals with looking from opposite directions through a 1962 Standard Atmosphere (ref. 24) to which temperature and pressure gradients have been applied. The second example is an attempt, using the new technique, to assess the qualitative effects of gradients on the analytical profiles in the winter flight of Project Scanner. The third example utilized the same body of data as the second example does, but shows how two

horizon detection techniques would be affected when looking at the same geographic area of tangent height from opposite directions.

Example 1

In example 1, these steps were followed:

(1) A 1962 Standard Atmosphere (ref. 24), containing no horizontal temperature or pressure gradients, was assumed. The resulting radiance profile appears in figure 2 and is listed as case A in table I.

(2) The atmosphere of step (1) was modified so that at all altitudes, temperature increased 0.5 kelvin per degree latitude toward the observer and the sea-level pressure gradient was assumed to be positive and of magnitude 1 millibar/degree latitude toward the observer. Note in figure 2 and in case B of table I that the radiance at low tangent heights exceeded that of step (1) by as much as 0.47 W/m^2-sr. This condition increases the peak radiance by 8.8 percent.

(3) Step (2) was repeated, the signs on the gradients therein being changed. This procedure simulated a look through the atmosphere in a direction opposite to that of step (2). Note in figure 2, and in case C of table I that the radiance at low tangent heights falls short of that in step (1) by as much as 0.46 W/m^2-sr. This condition decreases the peak radiance by 8.7 percent.

The results of steps (2) and (3) could be used, for example, in simulation of the difference in horizon signatures obtained if two horizon sensors were to look at the same geographic tangent area from opposite directions when the temperature gradients in the tangent height area are very strong over a great range of altitude.

Example 2

As mentioned earlier, the principal motivation for performing the present work was the inability, documented in reference 14, of the then-existing radiance computer program to handle the case encountered in the winter flight of Project Scanner, due to the existence of strong horizontal temperature gradients over the northern half of the scan area. These temperature gradients were not unusual, but are indeed rather characteristic of the winter season. The revised computational model was applied to the Project Scanner profiles to try to assess the improvement obtainable. Although the accuracy of the meteorological data obtained, and of the radiance measurements themselves, limit the conclusions which can be drawn (ref. 14), it is of interest to observe the comparison of the measurements with analytically derived profiles that used the modified program and estimated temperature and pressure gradients.

By meteorological analyses of the type described in appendix B, the horizontal temperature gradients along a typical line of sight from apogee (near Bermuda) to the region southwest of Hudson Bay were derived for the winter flight of Project Scanner. The temperature gradients at 1-km intervals from 0- to 80-km altitude for this case are listed in table II. These gradients are, on the average, smaller than those used in example 1, which was intended to be an extreme example. Two model atmospheres may be used to represent the atmospheric volume traversed by the line of sight for the winter flight of Project Scanner. One is constructed from meteorological data from Fort Churchill, Manitoba, and the other from data from Trout Lake, Ontario. The data from surface to 60 km at Fort Churchill were taken from rawinsonde and rocketsonde launches from that station. The data from surface to 30 km at Trout Lake are from a rawinsonde launch; above 30 km the data are the results of a thermal wind analysis, based on the rocket wind data from the Fort Churchill site. Because the line of sight of the radiometer scanned both in azimuth and in altitude through an atmosphere containing strong horizontal temperature gradients, it should not be surprising that the radiance profile observed cannot be assigned to any one location, as was possible in the summer flight which had very weak gradients. Also, radiometric errors, meteorological data errors, and analysis errors, the magnitudes of which are discussed extensively in reference 14, combine to make it rather difficult to make a positive statement that the new computational scheme improves agreement between theory and experiment. It can be hoped, however, that the correct trends are shown, when the new computational model is used. To determine the degree of improvement, figures 3(a) and 3(b) were drawn. Figure 3(a) shows that when the estimated gradients of table III were introduced, some improvement in agreement of theory with the Scanner measurement was obtained, especially at tangent heights of 10 to 20 km. Figure 3(b) shows Trout Lake model atmosphere radiances compared with the same Scanner measurement. It is interesting to note that although agreement at tangent heights less than 20 km is worse, better agreement is observed at tangent heights in excess of 25 km. The fact that there is better agreement with the Fort Churchill atmosphere, at low tangent altitudes, and better agreement with the Trout Lake atmosphere at higher tangent altitudes is encouraging. These agreements are in the correct sense because the atmospheric shell at tangent altitude is located further south (that is, toward Trout Lake) for the higher tangent altitudes, and further north for the lower tangent altitudes (that is, toward Fort Churchill) and, as mentioned before, the shell at the tangent height contributes a large part of the overall radiance. Another way of visualizing the changes brought about by the new technique is to extract from figures 3(a) and 3(b) the model radiances for Fort Churchill and Trout Lake from the previous model, together with the Fort Churchill curve from the new model, and plot them in figure 3(c). It is encouraging to note that the new Churchill curve fairs neatly from agreement with the old Churchill atmosphere at high altitudes to agreement with the

old Trout Lake curve at low altitudes. In summary, for this example, the technique has been applied to the only real data available for test. The error budgets in the radiometer data and meteorological data and analyses make impossible an exact evaluation of the technique. Nevertheless, it is very encouraging to note that the technique does shift the theory into better agreement with the observations, and in the correct sense.

Example 3

A final example of the utility of the technique is in the study, previously mentioned, of the stability of various horizon detection logic techniques. Reference 25 gives a thorough description of some of these techniques. The techniques of this reference are called "locators." Two of these locators are described briefly. Locator L1(X) denotes a technique which operates on a radiance profile to yield the tangent altitude at which the radiance level X W/m^2-sr is first encountered. Locator L3(Y) denotes a technique oper- ating on a radiance profile to yield the tangent altitude at which the radiance integrated over tangent height as the scan line moves inward from 80 km toward the solid earth and reaches the threshold Y W-km/m^2-sr. The locators L1(3.0) and L3(10.0) were used in this analysis, because they are believed to be readily implementable by horizon-sensor designers.

In this example, it is convenient to employ again the atmospheric data of the winter Project Scanner flight, as applied to the location Fort Churchill, Manitoba. These data certainly represent a physically realizable situation and should therefore give reasonable values for the variation in the located horizon detected by the two techniques.

By using the previous limb-radiance calculation approach, account is taken only of the atmosphere vertically above Fort Churchill, and no account is taken of the tempera- ture gradients existing between Fort Churchill and the observer. By this technique, the curve A of figure 4 is obtained. The effect of looking northward from the vicinity of Bermuda is simulated by the new radiance calculation approach; the gradients again are those given in table II. The radiance profile obtained is given by curve B. If the satellite is looking from the northwest of Churchill, so that the tangent point lies to its southwest- ward, toward Churchill, the radiance curve C is obtained. The located altitudes computed in the three cases are given in the following table:

Locator	Located altitude, km for –		
	Curve A	Curve B	Curve C
L1(3.0)	27.72	28.47	26.90
L3(10.0)	41.87	42.12	41.63

These altitudes should not be considered as either mean or extreme values of the differences to be expected when atmospheric gradents are included, but should be employed as an example of the differences that may be expected when a satellite looks at a location from different directions.

CRITERIA FOR USE OF GRADIENT MODEL

No firm criteria exist for selecting the conditions when the new model should be used in preference to that containing spherically symmetric atmospheres. Perhaps the best guide is the experience obtained in the summer and winter flights of Project Scanner. (See refs. 13 and 14.) In the summer flight, the symmetric model proved to be adequate. Figure 5 applies to the date of the summer flight. Thus, when gradients of the small magnitudes apparent from this figure exist, the symmetric model was adequate for the accuracy of the Scanner experiment. On the other hand, figure 6 shows the situation that existed in the winter flight. South of 20° north latitude, the old model was adequate; north of 45° north latitude, the gradients that appear in figure 6 are too large to allow accurate simulation of the radiance by the old model and require the use of the new one. The gradients appearing between 20° N and 45° N are in the transition region. Although it is difficult to give a general rule for deciding when the modified approach should be used, it appears that when horizontal temperature gradients exceed 0.4 kelvin per degree great circle throughout most of the atmosphere, the modified program should be used for a radiance accuracy of 1 percent.

CONCLUSIONS

A method is developed, using a numerical limb radiance computational model for the 14- to 16-micron CO_2 band, that accounts for the fact that real atmospheres strictly never show the spherically symmetric temperature and pressure stratification that is normally assumed in the calculations of limb radiance.

(1) The new technique has been implemented by modifying the Langley Research Center radiance model to include nonzero temperature and pressure gradients; the radiance profiles obtained have been physically reasonable in all cases.

(2) Equations have been presented, for the simple case wherein hydrostatic equilibrium is assumed to exist within the atmospheric volume of interest, to show how temperature and pressure gradients may be incorporated into any numerical limb-radiance computation model.

(3) The technique was applied to the atmospheric data for the winter flight of Project Scanner. The shape of the predicted radiance curve is believed to agree better with the experimental data than the shape predicted with the previous radiance computational model did.

(4) On the basis of the cases studied, differences between radiances predicted under the assumption of spherical symmetry and without the assumption can be significant under winter conditions at middle to subpolar latitudes.

Langley Research Center,
    National Aeronautics and Space Administration,
        Langley Station, Hampton, Va., July 28, 1969.

APPENDIX A

BASIC RADIATIVE TRANSFER THEORY

All the theoretical investigations of limb radiance have employed the well-founded theory of radiative transfer. (See refs. 26 and 27.) In these investigations, the thermal radiation from the atmosphere and the earth is integrated along the line of sight of the instrument by the summation of the radiative energy contributions from successively encountered spherically concentric shells. The radiation contribution from each shell is dependent on a source function containing the temperature of the shell, the frequency of the radiation, and the spectral transmissivity of the optically active gases.

When a band model is used to describe the absorption properties of the atmosphere, the transmission of each shell for a given narrow spectral interval is related mathematically to the optical path length, the effective temperature, and the effective pressure from the observing instrument to the shell. References 6 and 13 are instructive in understanding the geometry and physics of the radiance problem.

To give the basic radiative transfer equations which will be assumed to be known for the body of the report, the following mathematical discussion, adapted from reference 13, is presented here.

Radiative Transfer Equation

Any technique used to calculate the radiance profile of the earth's limb (refs. 2 to 12) has as a goal the solution of the radiative transfer problem in a curved atmosphere. The equation for radiance at a tangent height H is (from ref. 26):

$$N(H) = -\int_{\nu_1}^{\nu_2} \int_0^{S_0} J_\nu(T)\frac{\partial \tau}{\partial s}\, ds\, d\nu + \int_{\nu_1}^{\nu_2} J_\nu(T_0)\tau_0\, d\nu \tag{8}$$

where s_0, T_0, and τ_0 are the values at a boundary or for the last contributing layer of the atmosphere encountered in view along the line of sight of the instrument, when no boundary is present. The wave number limits of integration are denoted by ν_1 and ν_2. Tangent height is defined as the vertical distance along a geocentric radius vector from the surface of the earth to the point where the line of sight is normal to the radius vector. As long as the assumption of local thermodynamic equilibrium (refs. 26 and 27) is valid, the source function $J_\nu(T)$ is related to the Planck blackbody equation $W_\nu(T)$ as follows:

$$J_\nu(T) = \frac{W_\nu(T)}{\pi} = N_\nu(T) = \frac{C_1 \nu^3}{\exp\left(\frac{C_2 \nu}{T}\right) - 1} \tag{9}$$

15

Thus equation (8) can be rewritten as

$$N(H) = -\int_{\nu_1}^{\nu_2} \int_0^{S_o} N_\nu(T)\frac{\partial \tau}{\partial s} \, ds \, d\nu + \int_{\nu_1}^{\nu_2} N_\nu(T_o)\tau_o \, d\nu \qquad (10)$$

The second term of equation (10) represents a boundary condition determined by the temperature of the boundary and the fractional amount of that surface-induced radiation transmitted to the observer. If the tangent height is low enough to encounter them, it is also necessary to consider such physical boundaries as clouds and the earth's surface.

<div align="center">Solution of Transfer Equation</div>

In the transfer equation (eq. (10)) temperature is dependent on altitude, and transmittance is dependent on temperature, pressure, path length, concentration of absorbing gas, and wave number. The integrals of equation (10) are normally solved by numerical integration. It is convenient in solving equation (10) to rewrite it by changing the variables and limits of integration as

$$N(H) = -\int_{\nu_1}^{\nu_2} \int_{\tau_e}^1 N_\nu(T) \, d\tau \, d\nu + \int_{\nu_1}^{\nu_2} N(T_o)\tau_o \, d\nu \qquad (11)$$

In the first integral, $d\tau$ appears, integrated between τ_e (denoting the transmissivity from the last shell of atmosphere giving radiative contribution to the sum) and 1 (100 percent transmission of energy corresponding to the transmissivity from the shell nearest the observer beyond which none of the radiance emitted is absorbed). When spherical symmetry is assumed, a solution of equation (11) for a given tangent height is determined by the following step-by-step procedure:

(1) Divide the atmosphere into concentric spherical shells and find a mean temperature and a pressure representative of each shell

(2) Calculate a transmittance from the top of the atmosphere to each shell boundary for each band interval $\Delta\nu$

(3) Form the $\Delta\tau$ for each shell by subtracting one value of τ from the next value of τ

(4) Compute the blackbody radiance $N_\nu(T)$ for each shell by using the average temperature in the shell

(5) Sum the products $N_\nu(T) \, \Delta\tau \, \Delta\nu$ for the shells, and then sum over wave number. This step completes the solution.

This approach has been employed, to date, by all investigators using band models. To the author's knowledge, all previously computed theoretical radiance profiles have

APPENDIX A

employed model atmospheres wherein temperature changed only with altitude, or where such atmospheres were put in juxtaposition (ref. 11); these representations do not really represent the continuous gradients which actually exist in nature. These computed profiles have proven to be of great use for horizon-sensor design considerations, but more recently (ref. 14) have proven to be inadequate under conditions where strong horizontal temperature gradients exist (for example, in subarctic winter latitudes).

APPENDIX B

DETERMINATION OF PRESSURE AND TEMPERATURE GRADIENTS

It is desirable to be able to specify the horizontal gradients of temperature and pressure from the surface to 80 km over the geographic region of interest. The data for the altitude range of 0 to 30 km are readily available, at least in the northern hemisphere, in the form of facsimile copies of the constant-pressure-level analyses generated by Environmental Science Services Administration. These analyses also include temperature patterns. An example of this data is given as figure 7, which is a 700-mb analysis where the 3-digit numbers indicate the isolines of height of the 700-mb surface, as measured in decameters. Note that the height of the 700-mb surface is near 300 decameters or 3.0 km. The dotted lines indicate isotherms, lines of constant temperature. In figure 7, the temperatures range from -20° C to 5° C. The highest chart routinely analyzed on a synoptic or daily-use basis is that for the 10-mb surface (mean altitude, 31 km). Above this altitude, the Upper Air Branch of the National Meteorological Center of ESSA performs analyses on a less-frequent basis. (For example, see ref. 28.) Such analyses extend to 0.4 mb, or a nominal 54 km. The data above 30 km are derived from the firings of the Meteorological Rocket Network (MRN). (For example, see ref. 29.) Another way to obtain such analyses above 30 km is for the investigator to obtain the rocket data directly and to work with the wind and temperature data therein by using the thermal-wind analysis technique for constant-altitude surfaces (refs. 30 and 31) to obtain the isotherm patterns. After this procedure has been followed for a series of altitudes, the pressure-altitude profile may be constructed by use of the hydrostatic equation. After the pressure and temperature pattern is thus built up, cross sections similar to those derived for the flights of Project Scanner, and presented as figures 5 and 6, may be drawn. These cross sections allow the situation to be defined to an altitude of 55 km; the remainder of the atmosphere is difficult to define, because the useful rocketsonde data ceases near 55 km. One must employ either climatological atmospheres or meteorological judgment in describing the altitude interval of 55 km to 80 km.

APPENDIX C

TESTING THE MODEL

The new model was tested to determine whether it gives physically reasonable answers when various temperature and pressure gradients are entered into it. The following two tests were performed:

(1) Two atmospheres containing the same temperature structure were tested; only the horizontal pressure gradients were changed. The peak radiances should be the same. It is safest to perform this test on two isothermal atmospheres that have the same constant temperature and differ only in their surface pressures. Isothermalcy is required if effects of temperature change with altitude are not to enter the radiative transfer equation and to change the distribution of energy along the line of sight so much that the agreement of peak radiances would not be possible. The results are given in table III. Case I refers to a trial in which a 250° K isothermal atmosphere was input, with a surface pressure of 1010 mb, and the horizontal pressure gradients were set equal to zero. Case II refers to the same basic atmosphere as modified by the inclusion of a surface pressure gradient of 1 mb per degree great circle, toward the observer. All pressures aloft were constructed by hydrostatic buildup in both cases. Note that the maximum radiance occurred at a tangent height of -30 km. In case I, it was 7.7717 W/m^2-sr; in case II, it was 7.7718 W/m^2-sr. This difference amounts to only a 0.001-percent difference, and this result is within the basic 0.1 percent accuracy limitations in the radiance calculations. Therefore, the readings of cases I and II are to be considered as being the same, and test 1 is a success.

(2) Test 2 was performed to test the accuracy of the interpolation formulas for temperature and pressure, as applied to the basic spherically symmetric radiance calculation program and was as follows:

In an arbitrary case of nonzero temperature and pressure gradients, one tangent height low enough in the atmosphere to ensure that no energy was coming to the detector from beyond the tangent height point was chosen. The temperatures and pressures along this line of sight were computed. These computed values were inserted into the previous version of the model, which uses values as if they belong to a spherically symmetrical model atmosphere. The radiances were checked to make sure they were essentially the same. Use of a low tangent height was required, because it is impossible to include temperatures corresponding to the portion of the line of sight lying beyond the tangent height point in the symmetric model. If the tangent height is sufficiently low to allow the atmosphere to become opaque at or before the tangent point, the possible temperature ambiguity cannot arise.

APPENDIX C

The results of such a test are as follows. If temperature is changing 1 K per degree great circle at all altitudes from 0 to 80 km in such a way that the observer is always looking toward colder temperatures, and the sea-level pressure gradient is 1 millibar per degree of great circle, the radiance for a tangent height of 10 km is 6.3275 W/m^2-sr when calculated by the new model. If option 4 (see section entitled "Description of Original and Revised Models") is used to calculate interpolated temperatures and pressures and these values are substituted into the original (that is, spherically symmetric) radiance calculation program, the radiance for a tangent height of 10 km is 6.3262 W/m^2-sr. The agreement between these two numbers is thus within 0.02 percent. Therefore, it is again concluded that the test is passed within the basic accuracy of the radiance calculations.

In order to assess the added computation time which the modified computer program requires over that required by the original version of the program, both programs were used to process the same model atmosphere. The test case was the 1962 Standard Atmosphere, in 1-km increments up to 80-km altitude. (See ref. 24.) The radiances for 65 tangent heights were computed. The old model required 30 seconds, the new 56 seconds on the Langley Research Center computer complex (Control Data Corporation 6000 series). Thus, it is concluded that the time requirement is approximately doubled.

REFERENCES

1. Kirk, Raymond, J.; Watson, Bruce F.; Brooks, Edward M.; and Carpenter, Robert O'B.: Infrared Horizon Definition — A State-of-the-Art Report. NASA CR-722, 1967.

2. Kondratiev, K. Y.; and Yakushevskaya, K. E.: Angular Distribution of the Outgoing Thermal Radiation in the Different Regions of the Spectrum. First International Symposium on Rocket and Satellite Meteorology, H. Wexler and J. E. Caskey, Jr., eds., John Wiley & Sons, Inc., 1963, pp. 254-277.

3. McGee, R. A.: An Analytical Infrared Radiation Model of the Earth. Appl. Opt., vol. 1, no. 5, Sept. 1962, pp. 649-653.

4. Hanel, R. A.; Bandeen, W. R.; and Conrath, B. J.: The Infrared Horizon of the Planet Earth. NASA TN D-1850, 1963. (Also published in J. Atmos. Sci., vol. 20, no. 2, Mar. 1963, pp. 73-86.)

5. Woestman, John W.: Earth Radiation Model for Infrared Horizon Sensor Applications. Infrared Phys., vol. 3, no. 2, July 1963, pp. 93-105.

6. Wark, D. Q.; Alishouse, J.; and Yamamoto, G.: Calculations of the Earth's Spectral Radiance for Large Zenith Angles. Meteorol. Satellite Lab. Rep. No. 21, Weather Bur., U.S. Dep. Com., Oct. 1963.

7. Wark, D. Q.; Alishouse, J.; and Yamamoto, G.: Variation of the Infrared Spectral Radiance Near the Limb of the Earth. Appl. Opt., vol. 3, no. 2, Feb. 1964, pp. 221-227.

8. Duncan, John; Wolfe, William; Oppel, George; and Burn, James: Infrared Horizon Sensors. 2389-80-T (Contract NOnr 1224(12)), Inst. Sci. Technol., Univ. of Michigan, Apr. 1965. (Available from DDC as AD 466289.)

9. Burn, James W.: Infrared Horizons for Model Atmospheres of the Earth. Proceedings of the First Symposium on Infrared Sensors for Spacecraft Guidance & Control, Barnes Eng. Co., c.1965, pp. 3-14.

10. Burn, J. W.; Uplinger, W. G.; and Morris, P. P.: Earth Limb Radiance Profiles for the 15-Micron Carbon Dioxide Absorption Band — Data Computed by Month for Every 10 Degrees of Latitude in the Northern Hemisphere. LMSC 677318 (Contract AF 04(695)-1031), Lockheed Missiles & Space Co., Mar. 10, 1967.

11. Bates, Jerry C.; Hanson, David S.; House, Fred B.; Carpenter, Robert O'B.; and Gille, John C.: The Synthesis of 15μ Infrared Horizon Radiance Profiles From Meteorological Data Inputs. NASA CR-724, 1967.

12. Anon.: Compilation of Atmospheric Profiles and Synthesized 15μ Infrared Horizon Radiance Profiles Covering the Northern Hemisphere in the Longitude Region Between 60° W and 160° W from March 1964 Through February 1965. Honeywell, Inc., Oct. 1966.
    Part I. NASA CR-66184.
    Part II. NASA CR-66185.

13. McKee, Thomas B.; Whitman, Ruth I.; and Davis, Richard E.: Infrared Horizon Profiles for Summer Conditions From Project Scanner. NASA TN D-4741, 1968.

14. Whitman, Ruth I.; McKee, Thomas B.; and Davis, Richard E.: Infrared Horizon Profiles for Winter Conditions From Project Scanner. NASA TN D-4905, 1968.

15. Conrath, Barney J.: Earth Scan Analog Signal Relationships in the TIROS Radiation Experiment and Their Application to the Problem of Horizon Sensing. NASA TN D-1341, 1962.

16. Bradfield, L.: Horizon Sensor Infra-Red Flight Test Program. Rep. No. AO64189, Lockheed Missiles & Space Co., Oct. 19, 1962.

17. Collinge, J.; and Haynie, W.: Measurement of 15-Micron Horizon Radiance From a Satellite. EK/ARD ED-995 (Contract AFO4(695)-160), Eastman Kodak Co., Mar. 1, 1963. (Available from DDC as AD No. 437 804.)

18. McKee, Thomas B.; Whitman, Ruth I.; and Engle, Charles D.: Radiometric Observations of the Earth's Horizon From Altitudes Between 300 and 600 Kilometers. NASA TN D-2528, 1964.

19. Jalink, Antony, Jr.; Davis, Richard E.; and Hinton, Dwayne E.: Radiometric Measurements of the Earth's Infrared Horizon From the X-15 in Three Spectral Intervals. NASA TN D-4654, 1968.

20. Walker, R. G.; Cunniff, C. V.; and D'Agati, A. P.: Measurement of the Infrared Horizon of the Earth. AFCRL-66-631, U.S. Air Force, Sept. 1966.

21. Dodgen, John; and Curfman, Howard J.: Summary of Horizon Definition Studies Being Undertaken by Langley Research Center. Proceedings of the First Symposium on Infrared Sensors for Spacecraft Guidance & Control, Barnes Eng. Co., c.1965, pp. 233-239.

22. Dodgen, J. A.; McKee, T. B.; and Jalink, A.: NASA-LRC Program To Define Experimentally the Earth's IR Horizon. NASA paper presented at the Symposium on Infrared Horizon Sensors for Spacecraft Guidance and Control (El Segundo, Calif.), Mar. 14-15, 1967.

23. Anon.: U.S. Standard Atmosphere Supplements, 1966. Environ. Sci. Serv. Admin., NASA, and U.S. Air Force, 1966.

24. Anon.: U.S. Standard Atmosphere, 1962. NASA, U.S. Air Force, and U.S. Weather Bur., Dec. 1962.

25. Thomas, John R.: Derivation and Statistical Comparison of Various Analytical Techniques Which Define the Location of Reference Horizons in the Earth's Horizon Radiance Profile. NASA CR-726, 1967.

26. Goody, R. M.: Atmospheric Radiation. I.- Theoretical Basis. Clarendon Press (Oxford), 1964.

27. Kondrat'yev, K. Ya. (O. Tedder, trans.): Radiative Heat Exchange in the Atmosphere. Pergamon Press Inc., c.1965.

28. Staff, Upper Air Br., Nat. Meteorol. Center: Weekly Synoptic Analyses, 5-, 2-, and 0.4-Mb. Surfaces for 1964. ESSA Tech. Rep. WB-2, U.S. Dep. Com., Apr. 1967.

29. Anon.: Data Report — Meteorological Rocket Network Firings, vol. III, no. 12, World Data Center A: Meteorology, Nat. Acad. Sci.-Nat. Res. Council, Dec. 1966.

30. Petterssen, Sverre: Weather Analysis and Forecasting. Volume I — Motion and Motion Systems. Second ed., McGraw-Hill Book Co., Inc., 1956.

31. Peterson, Roy E.; Schuetz, John; Shenk, William E.; and Tang, Wen: Derivation of a Meteorological Body of Data Covering the Northern Hemisphere in the Longitude Region Between 60° W and 160° W From March 1964 Through February 1965. NASA CR-723, 1967.

TABLE I.- THE 1962 STANDARD ATMOSPHERE'S RADIANCE IN

THE 615- TO 715-cm^{-1} BAND, FOR THREE CASES OF
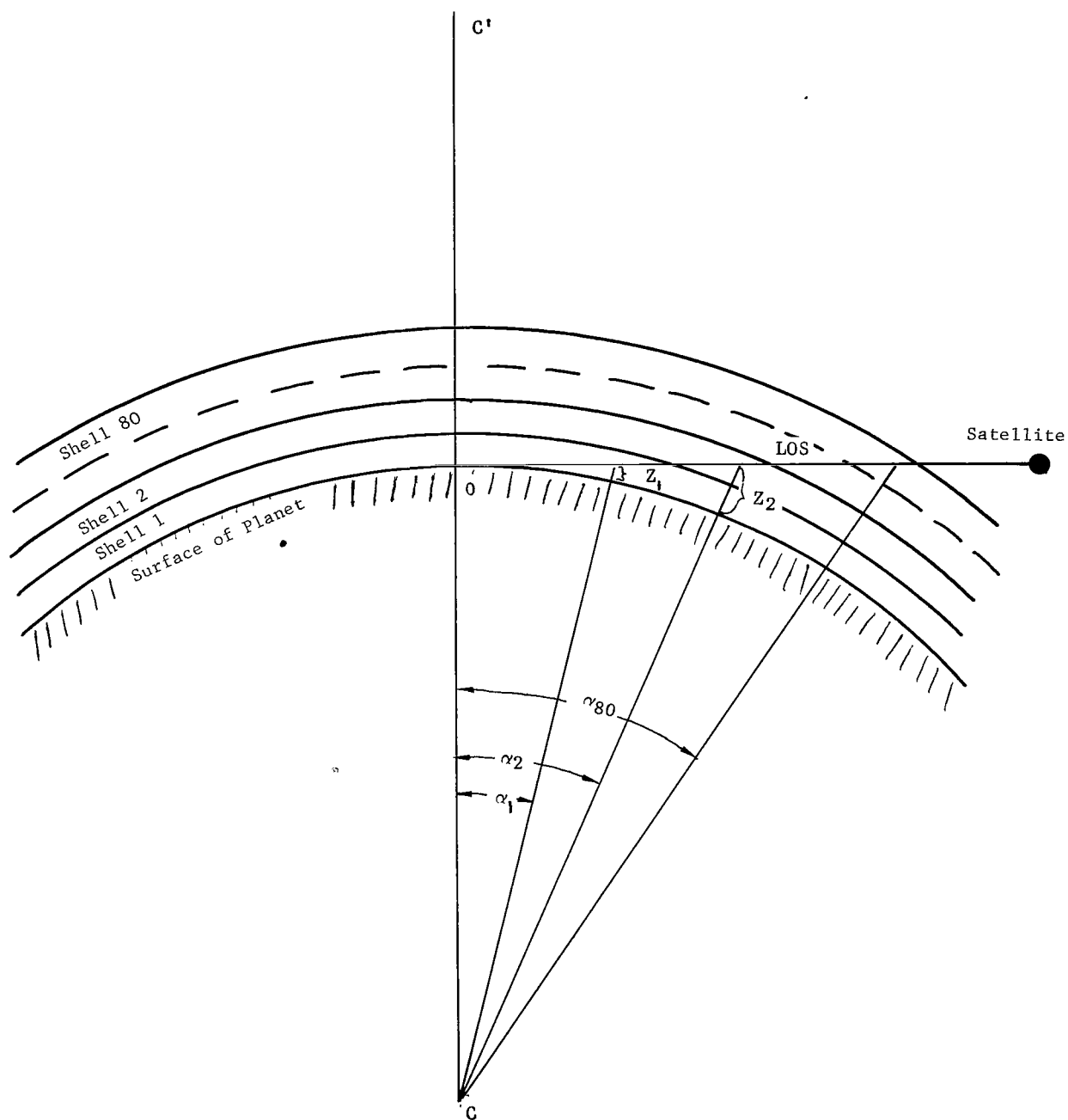
TEMPERATURE AND PRESSURE GRADIENTS

Tangent height, km	Radiance, W/m^2-sr, for —		
	Case A	Case B	Case C
0	5.3215	5.7868	4.8794
5	5.3372	5.8081	4.8909
10	5.3553	5.8311	4.9028
15	5.3705	5.8479	4.9178
20	5.2572	5.7293	4.8131
25	4.8938	5.3444	4.4764
30	4.1819	4.5912	3.8103
35	3.2991	3.6409	2.9949
40	2.3967	2.6588	2.1682
45	1.5959	1.7787	1.4402
50	.9348	1.0481	.8415
55	.4711	.5352	.4199
60	.2167	.2495	.1907

TABLE II.- HORIZONTAL TEMPERATURE GRADIENTS APPLIED TO

THE MODEL ATMOSPHERES SOUTHWEST OF HUDSON BAY

FOR THE WINTER 1966 PROJECT SCANNER MISSION

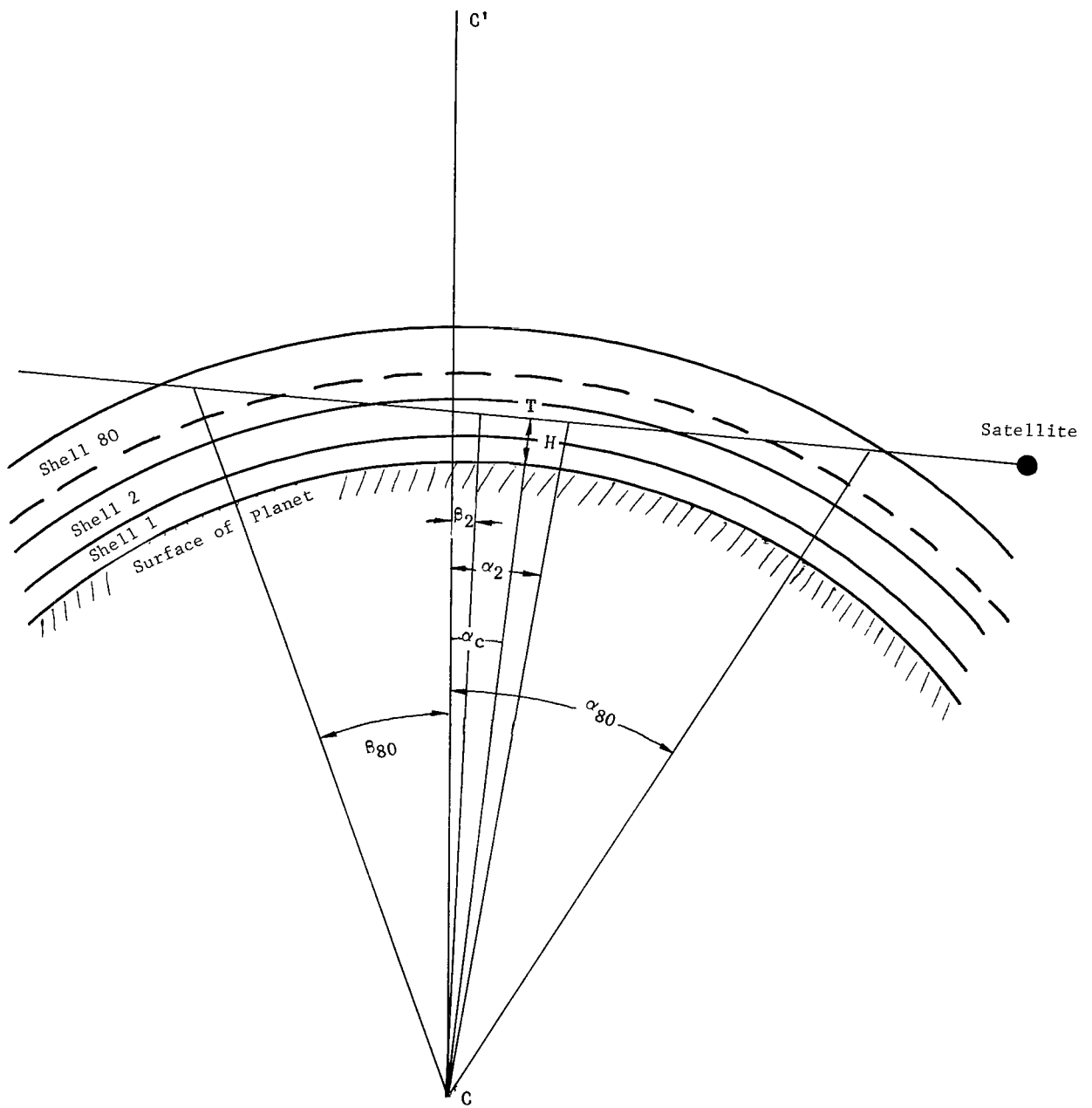| Altitude, km	Temperature gradient, K/deg great circle, southward
0	-0.6
1	-.2
2	-.4
3	.3
4	.2
5	.33
6	.5
7	.7
8	1.0
9	.3
10 to 11	-.1
12	-.2
13	-.15
14 to 16	-.5
17	-.4
18	-.2
19 to 20	0
21	.08
22	.15
23	.2
24	.03
25	.3
26 to 27	.4
28 to 31	.6
32 to 33	.7
34 to 36	.8
37 to 38	.9
39 to 40	1
41	1.1
42 to 43	1.2
44	1.3
45	1.4
46 to 50	.63
51	.5
52	.38
53	.25
54 to 81	.13

TABLE III.- RESULTS OF TEST I — TWO 250 K ISOTHERMAL ATMOSPHERES HAVING DIFFERENT PRESSURE GRADIENTS

Tangent height, km	Radiance, W/m^2-sr, for —	
	Case 1	Case 2
-30	7.7717	7.7718
-25	7.7716	7.7717
-20	7.7715	7.7716
-15	7.7715	7.7716
-10	7.7714	7.7715
5	7.7713	7.7714
0	7.7712	7.7712
5	7.7710	7.7710
10	7.7702	7.7702
15	7.7588	7.7587
20	7.6222	7.6216
25	7.0866	7.0852
30	5.9973	5.9956
35	4.4389	4.4372
40	2.9068	2.9058
45	1.7485	1.7480
50	.9974	.9972
60	.3098	.3099
70	.1128	.1129

(a) Line of sight tangent to the earth.

Figure 1.- Basic horizon-radiance viewing geometry.
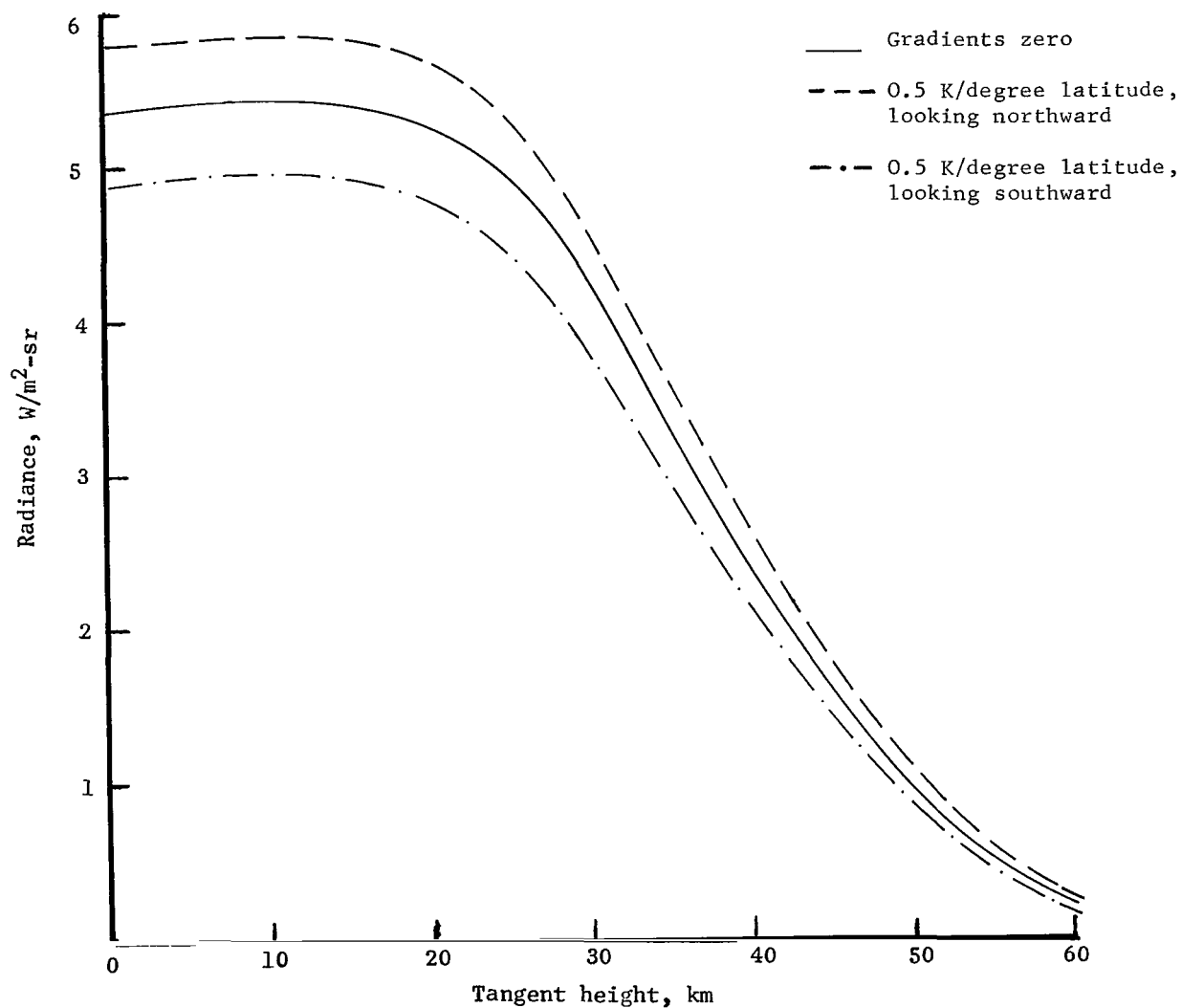
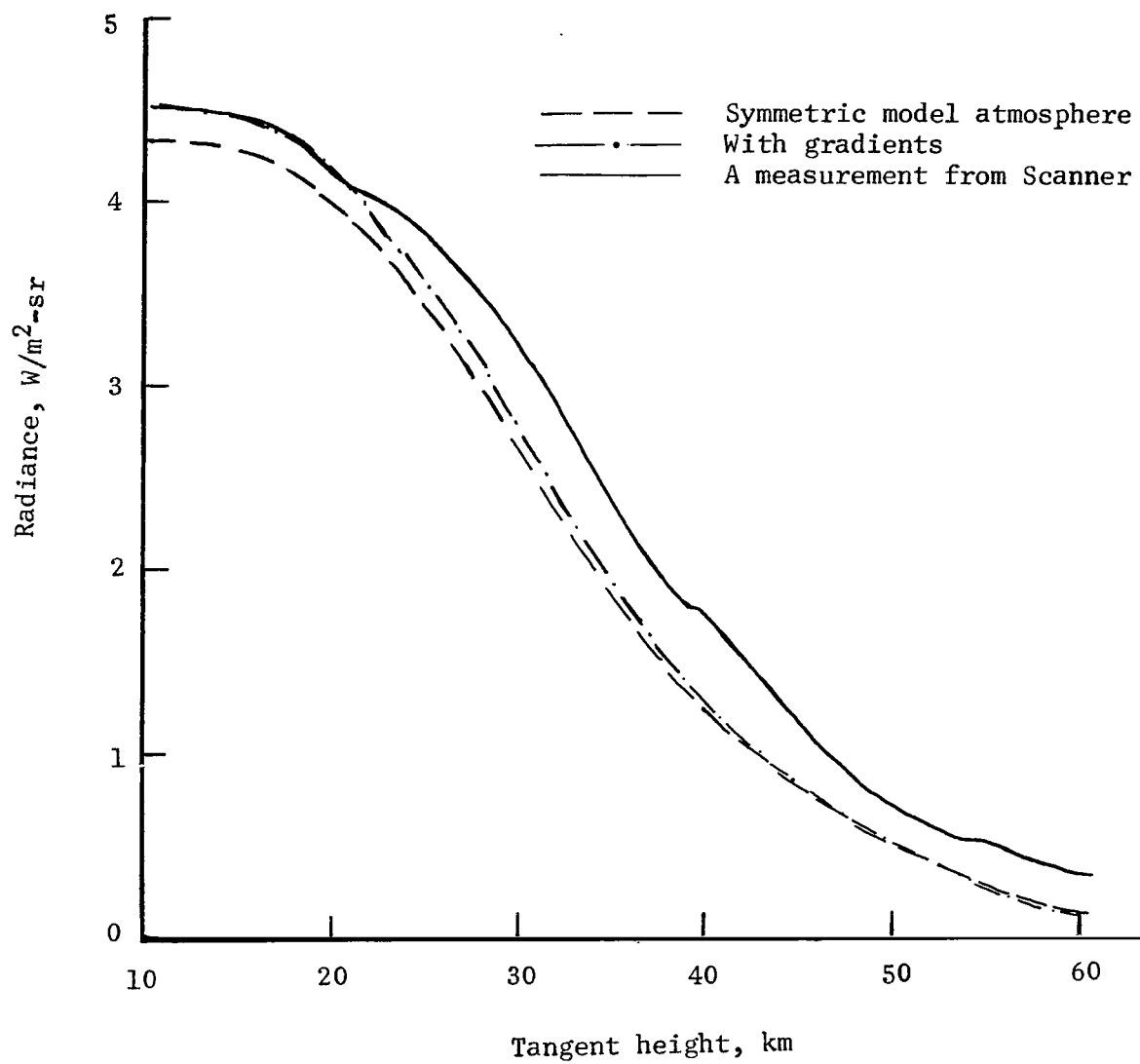(b) Line of sight above the earth.
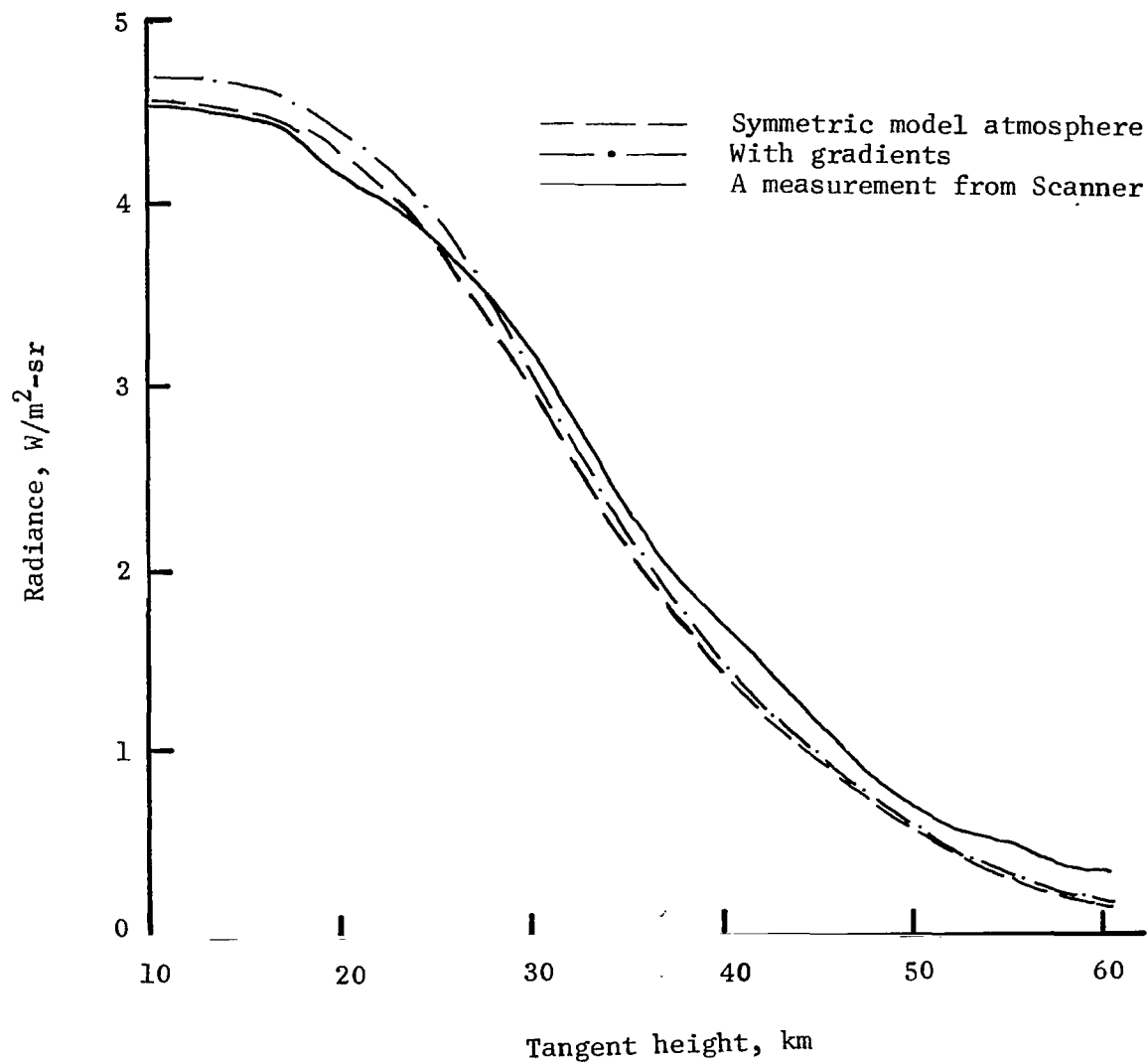
Figure 1.- Concluded.

Figure 2.- Effects on radiance profile of adding temperature gradients to the 1962 Standard Atmosphere.

(a) Model atmospheres for Fort Churchill.
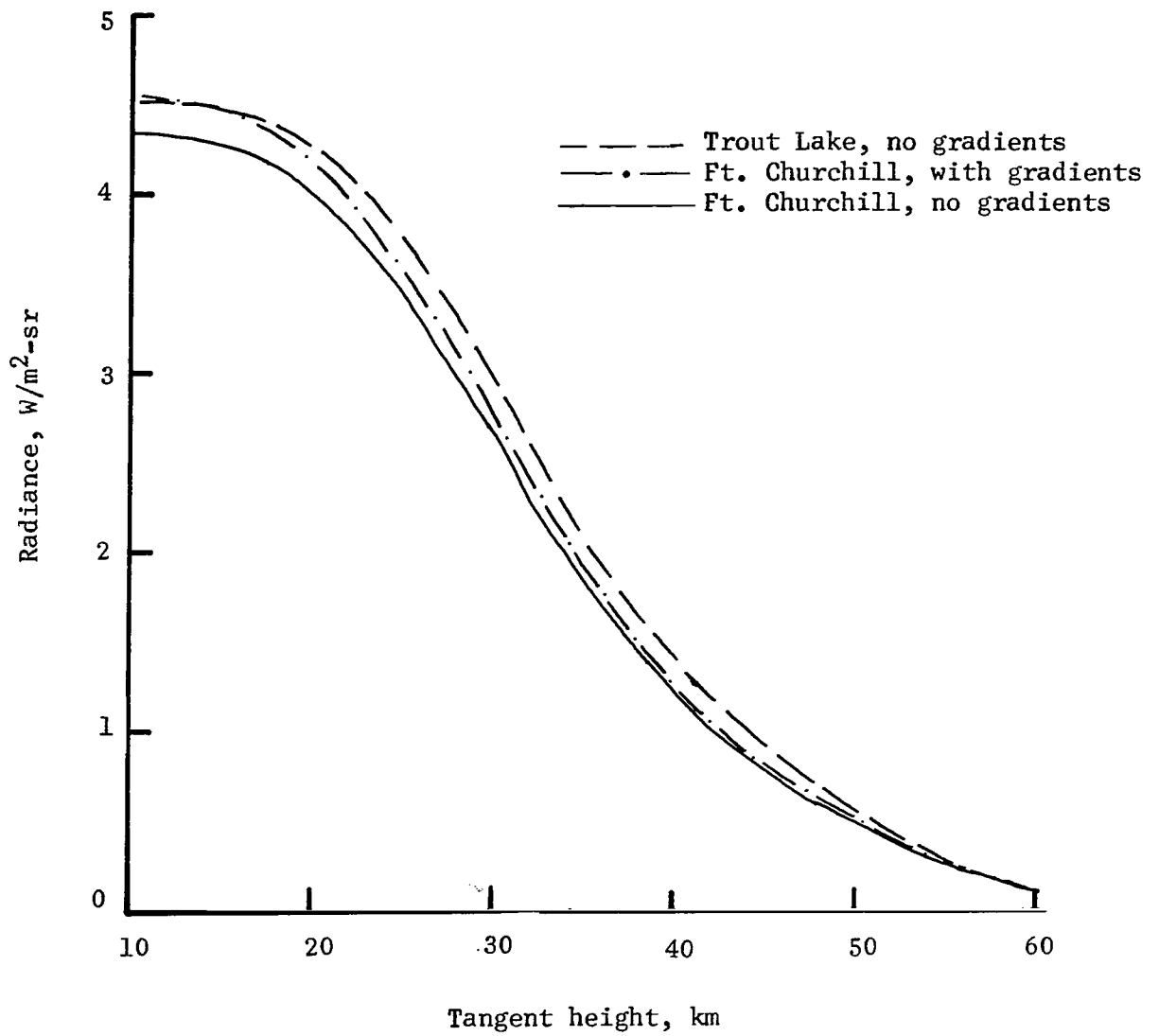
Figure 3.- Comparison of model atmosphere radiances (with and without gradients) with a Scanner-measured radiance profile.

(b) Model atmospheres for Trout Lake.

Figure 3.- Continued.

(c) Three model atmospheres compared.

Figure 3.- Concluded.

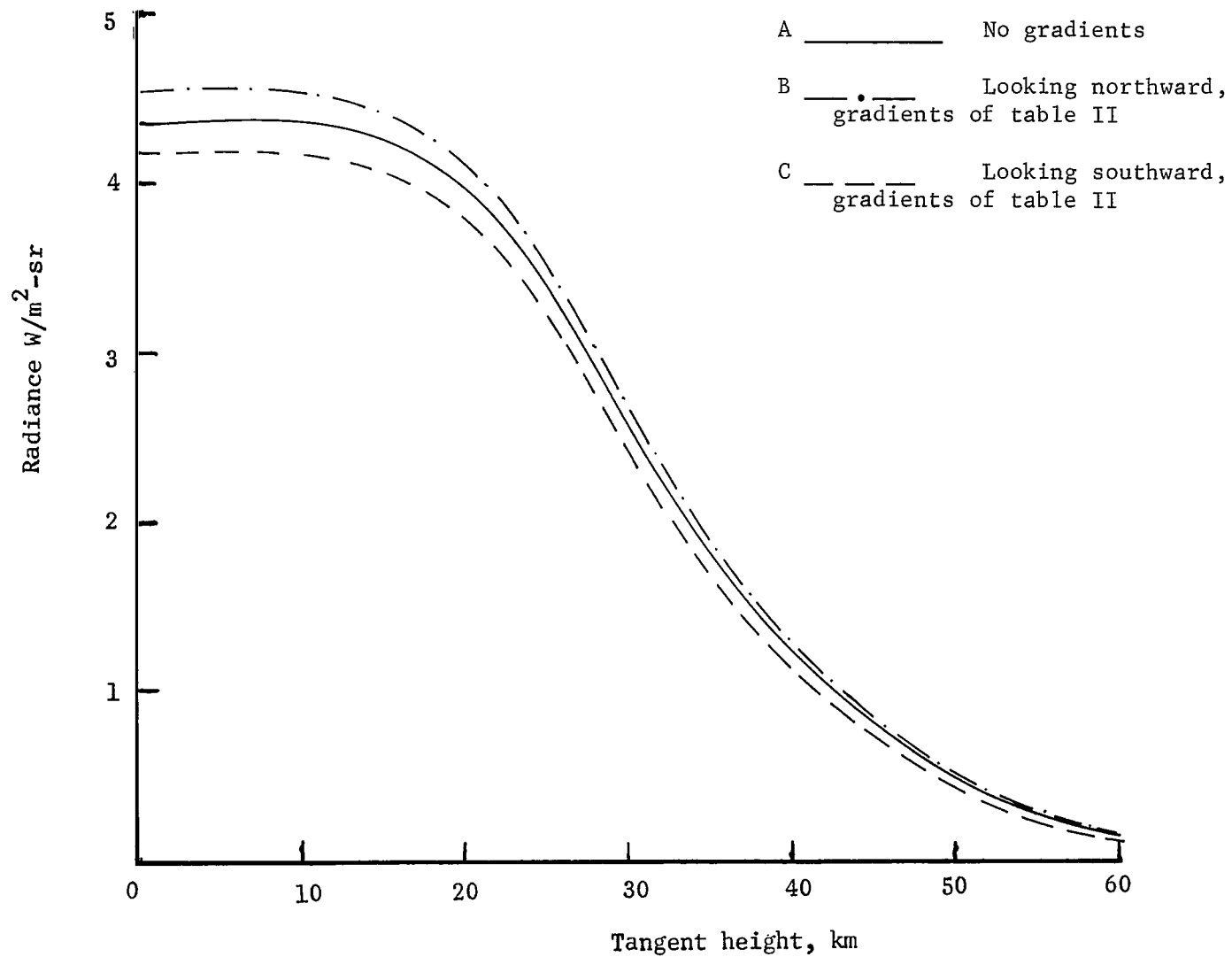Figure 4.- Effect of looking from opposite directions toward Fort Churchill in the presence of the temperature gradients given in table II.
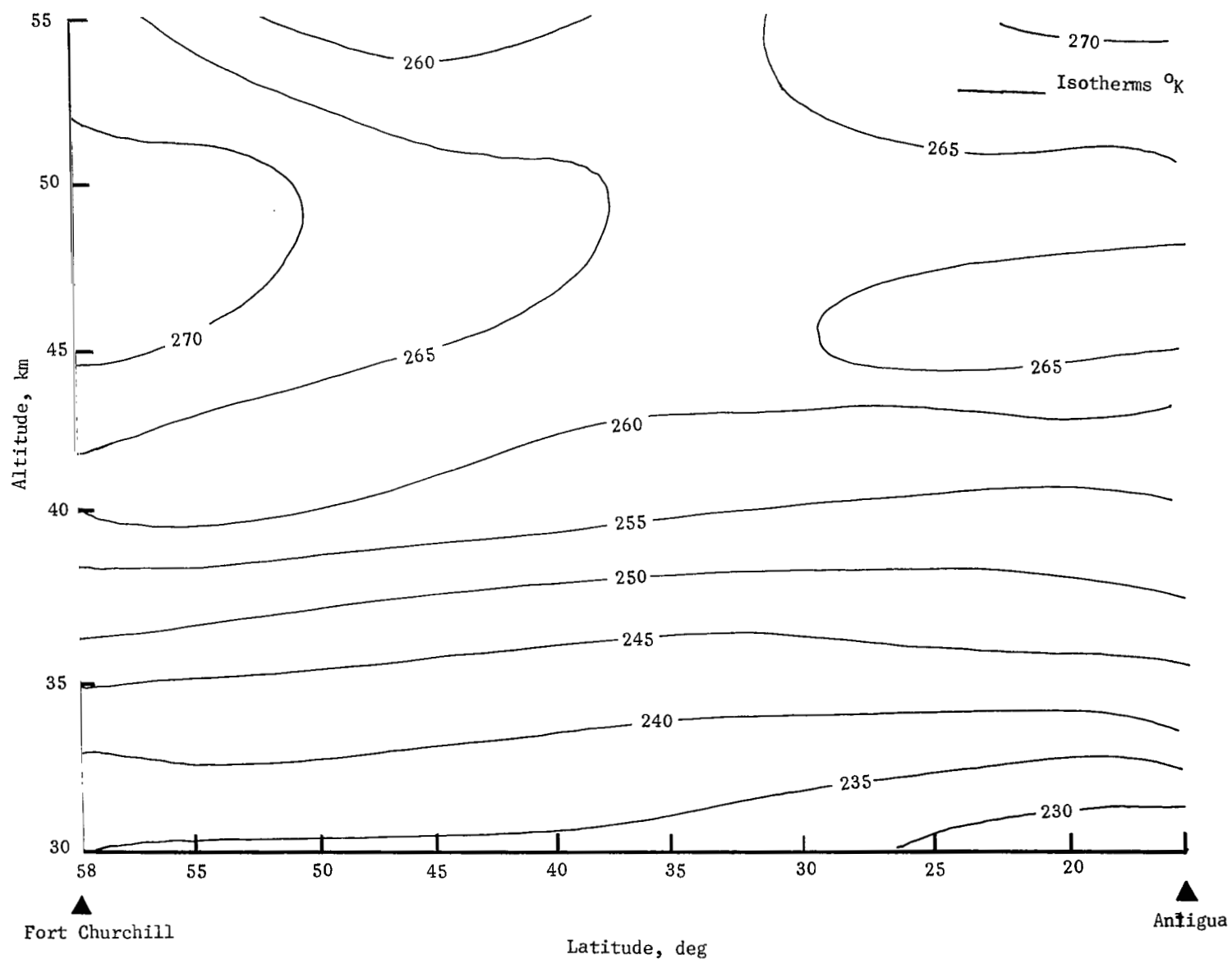
Figure 5.- Spatial cross-section temperature analysis Fort Churchill - Antigua 0600 hours GMT, August 16, 1966.
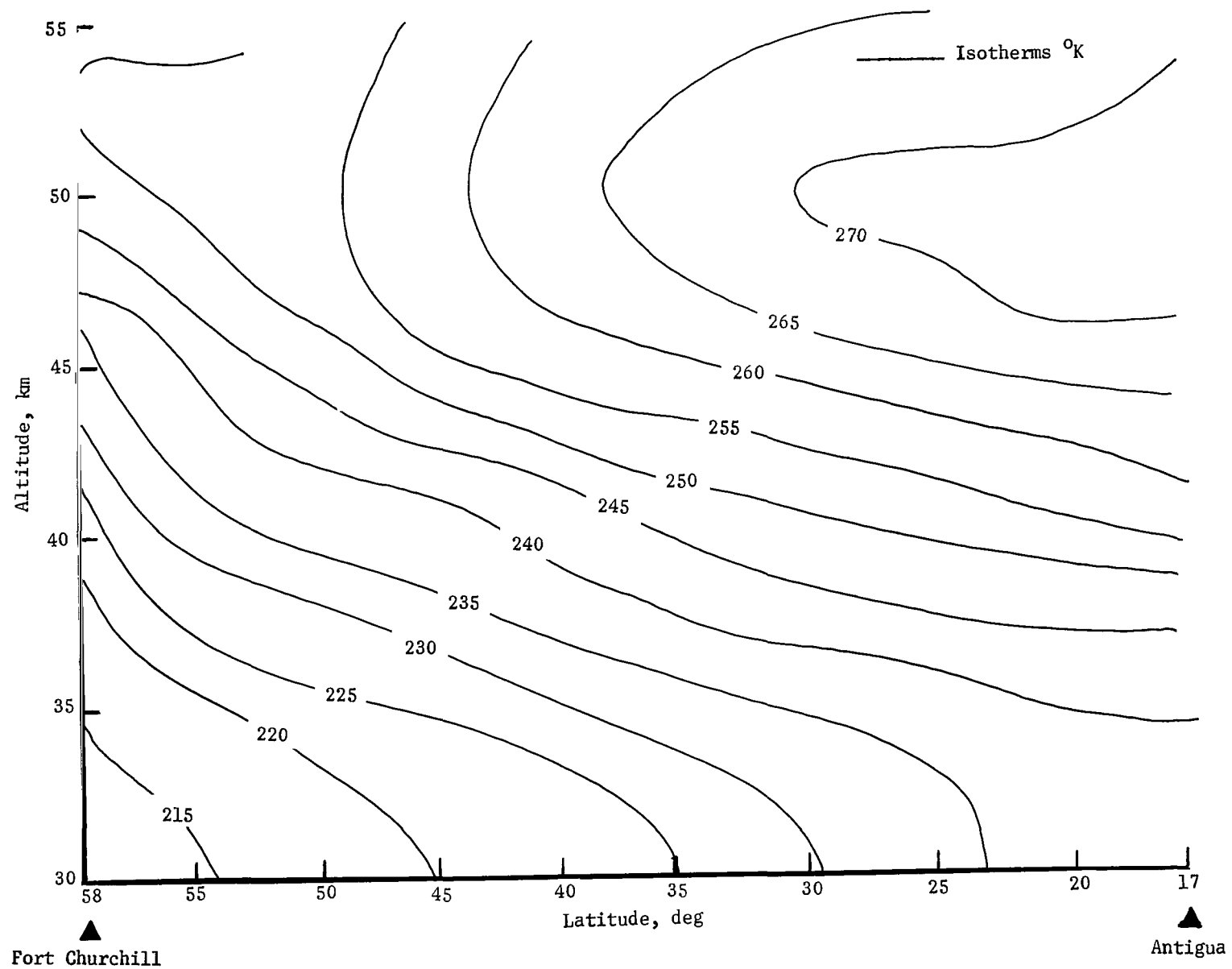
Figure 6.- Spatial cross-section temperature analysis Fort Churchill - Antigua 0600 hours GMT, December 10, 1966.
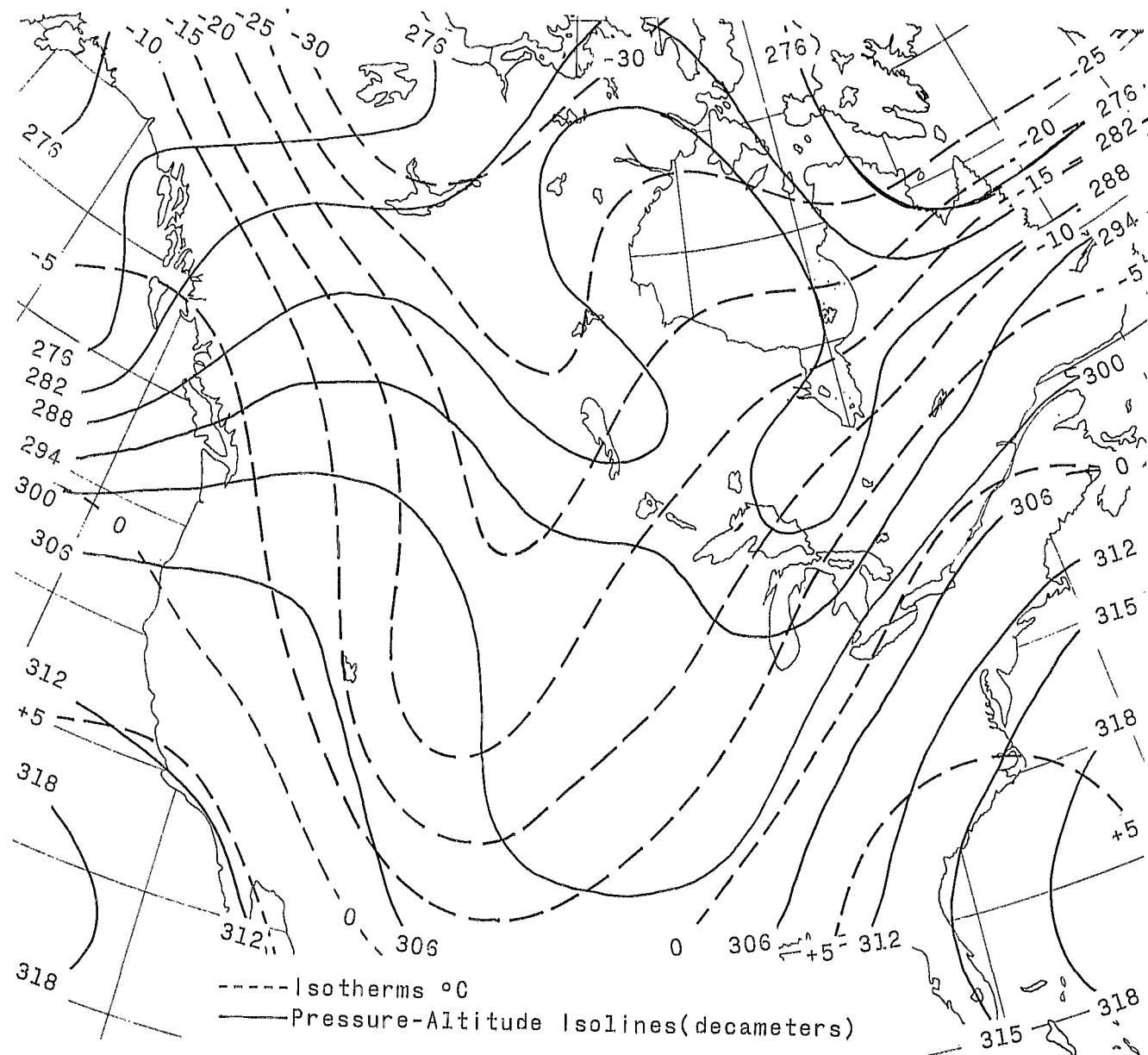
Figure 7.- Typical 700-mb chart (1200 hrs GMT, December 9, 1966).

FIRST CLASS MAIL

POSTMASTER: If Undeliverable (Section 158
Postal Manual) Do Not Return

"The aeronautical and space activities of the United States shall be conducted so as to contribute . . . to the expansion of human knowledge of phenomena in the atmosphere and space. The Administration shall provide for the widest practicable and appropriate dissemination of information concerning its activities and the results thereof."

— NATIONAL AERONAUTICS AND SPACE ACT OF 1958

NASA SCIENTIFIC AND TECHNICAL PUBLICATIONS

TECHNICAL REPORTS: Scientific and technical information considered important, complete, and a lasting contribution to existing knowledge.

TECHNICAL NOTES: Information less broad in scope but nevertheless of importance as a contribution to existing knowledge.

TECHNICAL MEMORANDUMS: Information receiving limited distribution because of preliminary data, security classification, or other reasons.

CONTRACTOR REPORTS: Scientific and technical information generated under a NASA contract or grant and considered an important contribution to existing knowledge.

TECHNICAL TRANSLATIONS: Information published in a foreign language considered to merit NASA distribution in English.

SPECIAL PUBLICATIONS: Information derived from or of value to NASA activities. Publications include conference proceedings, monographs, data compilations, handbooks, sourcebooks, and special bibliographies.

TECHNOLOGY UTILIZATION PUBLICATIONS: Information on technology used by NASA that may be of particular interest in commercial and other non-aerospace applications. Publications include Tech Briefs, Technology Utilization Reports and Notes, and Technology Surveys.

Details on the availability of these publications may be obtained from:

SCIENTIFIC AND TECHNICAL INFORMATION DIVISION

NATIONAL AERONAUTICS AND SPACE ADMINISTRATION
Washington, D.C. 20546